DOI: https://doi.org/10.37434/tpwj2024.09.03

NEUTRON SHIELD MATERIALS BASED ON BORON CARBIDE–TUNGSTEN MULTILAYER COMPOSITES

L. Chkhartishvili[1,2], N. Barbakadze[3], O. Tsagareishvili[2], A. Mikeladze[2], O. Lekashvili[3], K. Kochiashvili[3], R. Chedia[2,3]

[1]Georgian Technical University
77 Merab Kostava Ave., 0160, Tbilisi, Georgia
[2]F. Tavadze Metallurgy and Materials Science Institute
8b Elizbar Mindeli Str., 0186, Tbilisi, Georgia
[3]P. Melikishvili Institute of Physical and Organic Chemistry
31a Anna Politkovskaya Str., 0186, Tbilisi, Georgia

ABSTRACT

Nuclear power industry requires structural materials that effectively absorb neutron radiation. For this purpose, boron and boron-rich compounds and, in particular, boron carbide B_4C and its composites are widely used. Both theoretically and experimentally it has been shown that one such promising class of materials is boron carbide compositions with tungsten B_4C–W: tungsten phase inclusions containing heavy W atoms provide effective attenuation of the secondary gamma-radiation that accompany the absorption of primary neutrons by the boron ^{10}B isotope atoms. In this work, the composites with multilayer morphologies — $W/B_4C/W$, $W/B_4C/W_2B_5$, $W_2B_5/B_4C/W_2B_5$, etc. — in which boron carbide layers alternate with metallic tungsten and/or tungsten pentaboride ones, are produced and investigated. Surface metallization of boron carbide crystals or grains with tungsten powder, plate or coating is done by SPS (Spark-Plasma Sintering) and also by standard thermal sintering. SEM (Scanning Electron Microscopy) structural-morphological, XRD (X-Ray Diffraction) phase- and EDS (Energy Dispersive Spectrometry) chemical-compositions analysis of the obtained samples establishes that transition layers of W_2B_5 are formed on the B_4C–W interfaces, which ensures component-layers strong bonding.

KEYWORDS: boron carbide, tungsten, layered composite, metallization, thermal sintering, spark-plasma-sintering, radiation shield

INTRODUCTION

For structural materials effectively absorbing neutron radiation, nuclear power industry widely uses boron-rich compounds and composites, in particular, boron carbide B_4C and its composites with metals and other ceramics. Experimentally [1–5] and theoretically [6–9] it has been demonstrated that one of such promising class of materials is boron carbide compositions with tungsten B_4C–W. Tungsten and/or tungsten compounds phases, which contain heavy W atoms, provide effective attenuation of the secondary gamma-radiation that accompany the absorption of primary neutrons by the boron ^{10}B isotope nuclei. Composites with (poly-sandwich or multilayer morphologies — $W/B_4C/W$, $W/B_4C/W_2B_5$, $W_2B_5/B_4C/W_2B_5$, etc. — in which boron carbide layers alternate with metallic tungsten and/or tungsten boride ones, were produced and investigated.

As known, tungsten- and boron-based thin films, including B_4C, as well as tungsten carbide WC and boride WB_3, display very high hardness [10]. To expand the superior room-temperature mechanical properties of tungsten foils, the W-containing metallic laminate composites were fabricated [11]. The effect of neutron irradiation on W foil could be investigated to determine their resulting DBTT (Ductile-to-Brittle Transition Temperature) shift. Physical properties, processing techniques, and applications of high-operating temperature (> 1200 °C) materials with multi-layered ceramic/carbon, ceramic, and metal structures were highlighted in [12]. They may have a graceful failure mode and higher toughness as compared to particle-reinforced ceramic composites and, as multi-layered shields, provide better efficacy than single-layered ones. Work [13] aimed to describe the development of an online platform to calculate (in the energy range of 0.015–15 MeV) the 36 GSPs (Gamma Shielding Parameters), which are required to investigate the materials gamma-ray shielding.

The influence of interface roughness on the reflectivity of B_4C–W multilayers varying with bi-layer number N was specially investigated [14]. For such multilayers, fabricated by the DC (Direct Current) magnetron sputtering method, with the same design period thickness of 2.5 nm, a real-structure model was used to calculate the reflectivity variations with $N = 50$, 100, 150 and 200 bi-layers. Their reflectivity and scattering intensity measured by the XRD (X-Ray Diffraction) indicate that reflectivity is a function of N and interface roughness slightly increases from layer to layer in process of multilayer growth.

Coating different types of surfaces with metallic tungsten is used in several modern technologies. In particular, tungsten layer can be obtained [15] by tungsten oxide WO_3 layer formation using the spin coating to reduce it to α-W phase in a hydrogen atmosphere at 600–800 °C. With the aid of chemical vapor transport of $WO_x(OH)_y$, surface morphology is transformed into rod-like, star-shaped cracking, florets, irregularly fibrous structures and, finally, spherical tungsten particles. Usually, semiconductors are coated with a thin layer of tungsten, which is mainly carried out by the CVD (Chemical Vapor Deposition) method, where SiH_4, H_2 and WF_6 are used as precursors, and the vacuum chamber is maintained at pressures of about 20 to 760 Torr to improve the tungsten deposition rate [16]. Tungsten thin film was deposited on Si(100) substrate by using the LPCVD (Low Pressure CVD) technique [17, 18] also using WF_6 and SiH_4 as source and W-reducing gases, respectively.

Pure-W metallic films are often deposited not only by CVD, but also by PVD (Physical Vapor Deposition), by sputtering or evaporation. To avoid the chemical or physical methods drawback of using expensive high-vacuum instrumentation, metallic tungsten in form of thin film was reduced [19] from the water-soluble W–IPA (Inorganic Peroxopolytungstic Acid) composite powder prepared by dissolving metal tungsten in hydrogen peroxide and evaporating the residual solvent. Commonly, metallic tungsten deposition technologies on metal substrates applies [20] aluminum Al, copper Cu and titanium Ti. Deposition by ALD (Atomic Layer Deposition) and PNL (Pulsed Nucleation Layer) techniques may also be used to form tungsten nucleation layers. In industrial conditions, the evolution of the reduction process of tungsten blue oxides ultrafine powder to tungsten thin films under a counter-current flow of hydrogen is described [21] by the following scheme: $WO_{2.90} \rightarrow$ $\rightarrow WO_{2.72} \rightarrow WO_2 \rightarrow W$. It was developed [22] the HWALD (Hot Wire-Assisted ALD) to form W with its filament heated up to 1700–2000 °C in the flow of atomic hydrogen H generated by the dissociation of molecular hydrogen H_2, which reacted with WF_6 at the substrate to deposit.

One of the practical and cheap methods is that metallic tungsten is coated on the ceramic material using [23] the chemical solution deposition to fabricate such films on the inner surface of alumina tubules. This technique involves the preparation of tungsten oxide layers from PTA (PeroxoTungstic Acid) precursor solution and their subsequent reduction to tungsten in the presence of hydrogen. The suitability of using W-matrix coating materials supersaturated with B for stainless steel substrates was tested [24] and all the W–B coated (including W–13 % B and W–23 % B) materials are found to be nearly an order of magnitude more resistant to material loss through corrosion–wear compared to uncoated substrates.

As for the boron carbide–metal B_4C–Me, Me = Mo, W, Ni, etc., sandwich structures in general, they can be obtained by the boron carbide ceramic metallization method [25], which comprises the following steps:

- mixing the metals powder, for example, 10–40 wt.% of Mo, W and Ni, according to their weights ratio, carrying out ball milling, and sieving through 300-mesh sieve;
- preparing paste by mixing the metal powder obtained in the Step 1 with 5 wt.% ethylcellulose solution according to weight ratio of (100–120):30;
- printing the metalized paste obtained in the Step 2 on the 20–30 μm thick boron carbide ceramic part, needing to be metalized, and drying it; and
- metalizing by putting the boron carbide ceramic part dried in the Step 3 into a sintering furnace, introducing hydrogen, keeping the temperature at 1650–1680 °C for 30–35 min, keeping the dew point at 0–10 °C, and cooling along with the furnace.

The formed Mo–W–Ni proportioned metalized layer alloy material to have thermal expansion close to that of B_4C. Then, the bonding strength is high, the metalized stress is small, and due to the sub-μm metal network structure, the metal is not prone to falling off after being brazed.

A method of synthesizing B_4C coatings of metal substrates by using RF (Radio Frequency) plasma source with an external magnetic field is described in [26]. The nanohardness of coated steel surfaces is found in the range of 14.0–16.6 GPa and the B_4C coatings with 1.73–3.89-times higher hardness than uncoated (bare) steels serving as targets. This technique seems useful also for B_4C-coating of W substrates.

In this work, composites with multilayer morphologies — $W/B_4C/W$, $W/B_4C/W_2B_5$, $W_2B_5/B_4C/W_2B_5$, etc. — in which boron carbide B_4C layers alternate with metallic tungsten W and/or tungsten pentaboride W_2B_5 ones, are produced and investigated. The surface metallization of boron carbide crystals or grains with tungsten (*a*) powder, (*b*) plate or (*c*) coating (formed by peroxpolytungstic acid aqueous solution treatment at 600 °C in hydrogen flow) is done by SPS (Spark-Plasma Sintering) at temperature of 1300–1700 °C and pressure of 20–40 MPa for 6–10 min. Such layered composites are also obtained by standard thermal sintering (at temperature of 1300–1500 °C in argon atmosphere or vacuum) of the components bonded with organic compounds aqueous solutions containing 0.5–1.0 % boric acid. SEM

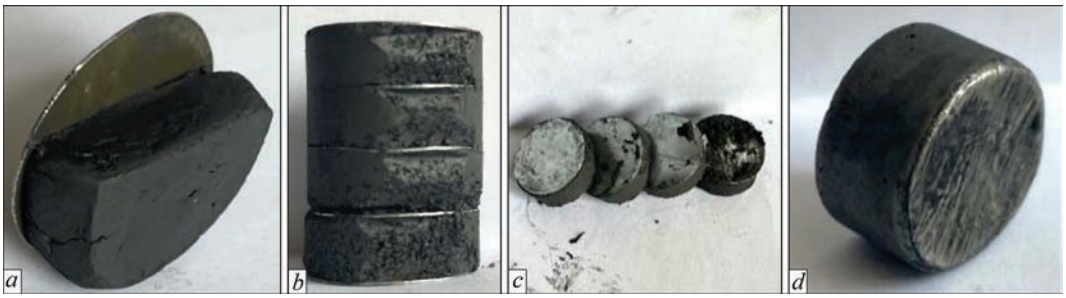

Figure 1. B_4C/W composite sandwich-like structures fabricated from tungsten plate and boron carbide powder: raw (*a*) monosandwich, (*b*) polysandwich and (*c*) its sections, and (*d*) sandwich-like structure produced by SPS at 1500 °C

(Scanning Electron Microscopy) structural-morphological, XRD phase- and EDS (Energy Dispersive Spectrometry) chemical-compositions analysis of obtained samples has established that transition layers of W_2B_5 are formed on the B_4C/W interfaces ensuring the strong component-layers bonding.

OBTAINING OF RAW SANDWICH-LIKE STRUCTURES

We have developed some new methods for obtaining the raw B_4C/W sandwich-like structures. As a tungsten source, tungsten powder and plate are used. Initial tungsten powder is obtained by dissolving tungsten scrap in 15–25 % solution of hydrogen peroxide. PTA is obtained by filtering and drying the solution. By its reducing with hydrogen at 500–600 °C for 4 h, it is obtained the tungsten powder. Both commercial boron carbide and tungsten pentaboride powders, and boron carbide matrix ceramic powders previously synthesized by authors from available inexpensive reagents, are used to prepare these sandwiches.

Here is described the synthesis method for PTA. 5.0 g of tungsten powder is slowly dissolved in 40 ml of 20–25 % H_2O_2. The H_2O_2 solution is added to the tungsten powder in 3 portions during 2 h (Note: The reaction is very exothermic!). Then, 15 ml of hydrogen peroxide solution is added to the reaction mixture again and stirred at room temperature for 5 h. The solution is left for 12 h and then filtered. A yellowish transparent solution is obtained. Excess H_2O_2 is decomposed using a platinum spiral and the solution is evaporated under vacuum. An orange crystalline substance containing 85.4 % tungsten oxide WO_3 is obtained. The sample is heated at 600 °C for 4 h.

As for other liquid-charge chemical synthesis methods that also are used here, they are described elsewhere [27–31]. These methods, previously developed for multi-component B_4C-matrix ceramics containing W compounds, have been modified for the purpose of obtaining B_4C–W layered composites.

The manufacturing technology of B_4C–W layered composite and corresponding (poly)sandwiches is illustrated in Figure 1. First, a paste of boron carbide is prepared using ethylcellulose 1 % solution for binding material, which also contains 0.5–1.0 % boric acid. Tungsten plate discs and B_4C wet (partially dried) powder are then placed alternately in the press-form. After pressing (at 5–10 atm) of the composite, the raw product is dried at room temperature and further processed by SPS at temperature of 1300–1700 °C and pressure of 20–40 MPa for 6–10 min. The thickness of the plates and the neutron absorbing material layers placed between them, as well as the total number of layers are variable.

The powder filling placed between the plates can be composite, consisting of several components. For example, it can be enriched with boron, tungsten, tungsten borides, etc. Some of the sandwiches we made contain 10–30 wt.% W and W_2B_5. Figures 2–4 show diffrectograms of initial powders. In the boron carbide commercial powder diffractogram, there are visible 3 intense B_4C peaks at 2θ = 23.5, 34.8 and 37.7°. In addition, there are also detected the traces of B_6C, $C_{12}BO_2$ and $C_{14}BO_2$ phases. Diffractogram of mixture of boron carbide and tungsten powders shows only 2 of 5 known peaks of W (40.4, 58.4, 73.3, 86.9 and 100.8°): 2θ = 40.4 and 58.4°. In addition to B_4C and W phases, there are also detected the traces of WB_4, W_5O_{14}, WO_3 and WO_4. Peaks of W_2B_5 phase visible in the diffractogram of mixture of boron carbide and tungsten pentaboride powders are placed at 2θ = 25.5, 35.3, 39.9 and 52.7°. In this case, besides main components B_4C and W_2B_5, there is detected a number of trace phases: W, WB_2, WB_4, WC, WO_2, $W_{18}O_{49}$, WO_3, W_3O_{10}, WO_4 and $C_{14}BO_2$.

By a similar method, sandwich composites can be obtained from tungsten and boron carbide powder pastes. In this case, the tungsten powder paste is placed in the mold and pressed with a punch so that the paste does not come out. Then they are added with wet powder of the neutron absorbing (composite) ma-

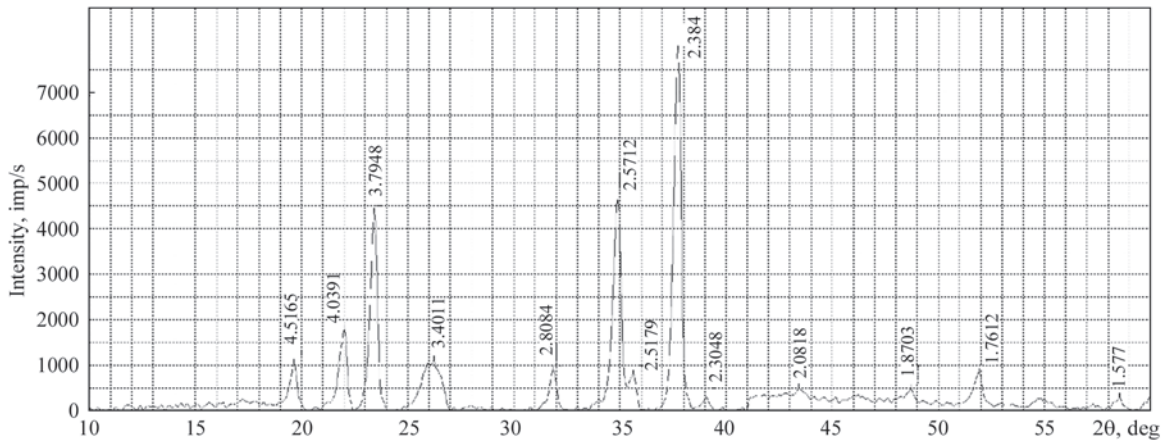

Figure 2. Boron carbide commercial powder diffractogram

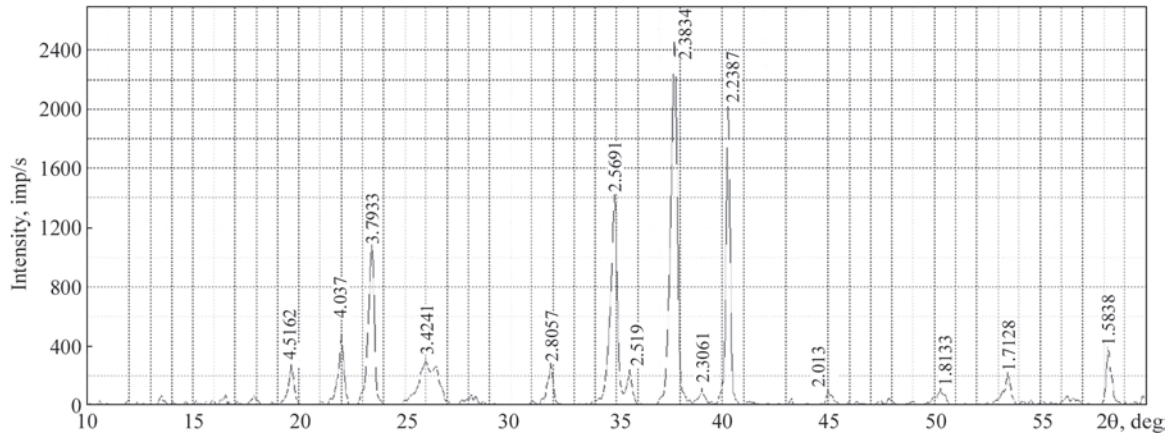

Figure 3. Diffractogram of mixture of boron carbide and tungsten powders

terial and pressed again. An image of the resulting section is shown in Figure 5.

In the next step, these intermediate products should compacted using a sintering method.

DETAILS OF SINTERING METHODS

used to obtain the sandwich-like B_4C/W composites are given below.

For the SPS compacting of W and B_4C powders, the 12 mm diameter graphite press-form lined with graphite foil is placed with a certain amount of commercial W powder and pressed with a punch. Boron carbide powder is added on top of the tungsten powder, which is also pressed with a punch to smooth the surface of the deposited powder. This surface is covered with graphite foil and a graphite punch is placed on top. The pressform is placed in the SPS equipment chamber, and, after its vacuuming, the powder is pressed at 30–50 MPa at temperature 1500–1700 °C for 10 min holding time. Pulsed AC (Alternating Cur-

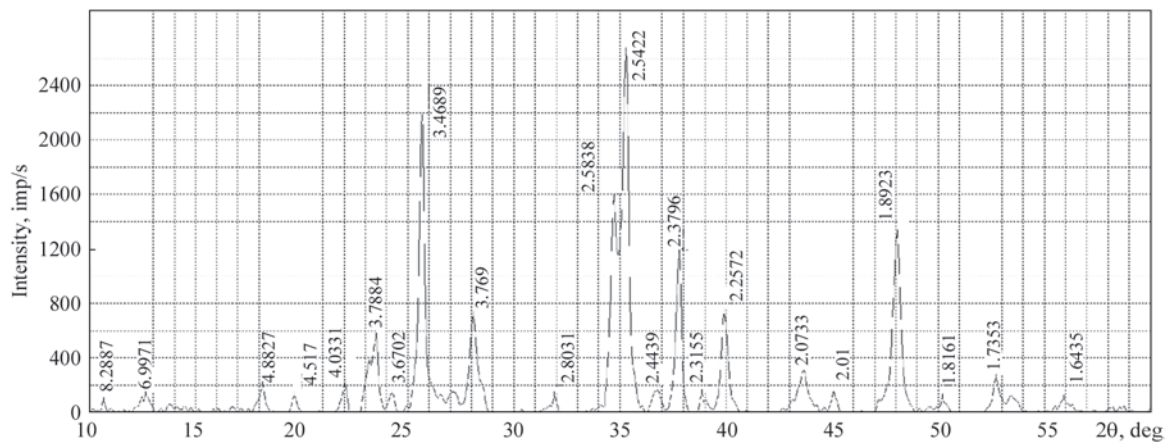

Figure 4. Diffractogram of mixture of boron carbide and tungsten pentaboride powders

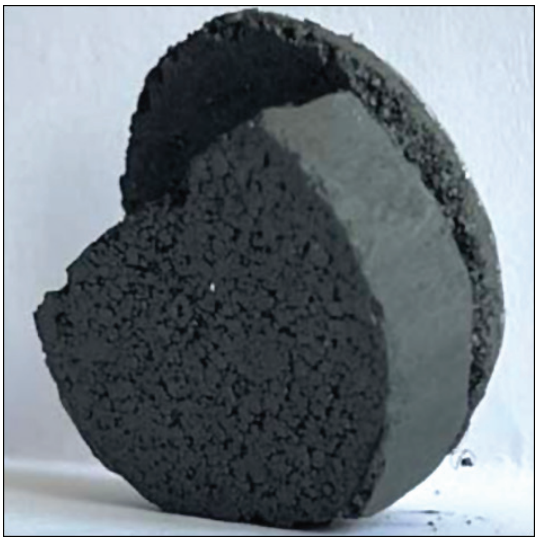

Figure 5. Sandwich made of tungsten (thin) and boron carbide (thick) powder paste layers

rent) mode with pulse duration of 5 μs and pause of 1 μs is used to sinter these ceramics. The sample heating rate reaches 100–200 °C/min. They are cooled in vacuum. Sandwich-like B_4C/W composites are obtained, where the boundary layer between components is well observable.

As for the SPS compacting of W foil and B_4C powder, for its conducting a tungsten disk of 12 mm diameter and thickness of 1–2 mm is placed on a graphite press-form of the same diameter lined with graphite foil and poured with boron carbide powder on top, and pressed with a punch to smooth the surface of the poured powder. Then, the surface is covered with graphite foil and a graphite punch is placed on its top. Sintering is carried out similarly to the described above. The samples are cooled in vacuum. Sandwich-like B_4C/W composites are obtained, where the boundary layer between two components is formed.

The following technological and measuring equipment and devices have been used for realization of above described processes.

To grind the powders there is used planetary mill Pulverisette 7 Premium Line with grinding cup and balls made from WC–Co hard alloy. For the ultrasound treatment and homogenization of suspensions is used an ultrasonic cleaner (45 kHz) and JY92–IIDN Touch Screen Ultrasonic Homogenizer (20–25 kHz, 900 W). Compaction of powder samples or simultaneous synthesis and compaction are carried out by using the SPS equipment manufactured at the Georgian Technical University (with an ability to operate in DC, pulsed DC and pulsed AC modes). Thermal treatment (< 1500 °C) of simples is implemented in high-temperature vacuum furnace Kejia.

X-Ray XRD patterns are obtained with DRON–3M (CuK_α, Ni filter, 2°/min) and XZG–4 (CuK_α, λ = 1.5418 Å) diffractometers. Morphology and microstructure of the powders are studied with SEM JEOL–JSM 6510 LV equipped with energy Dispersive Micro-X-Ray Spectral Analyzer X-MaxN (Oxford Instruments). Particles size of the powders are determined by the Scherrer method and also by photon correlation nanoparticle size analyzer Winner 802 DLS and Malvern Instruments Mastersizer. The specific surface area of the composite powder is measured on a Micromeritics Gemini VII Instrument.

CURRENT DEVELOPMENTS

Such layered composites also can be obtained by standard thermal sintering at temperature of 1300–1500 °C in argon atmosphere or vacuum from the components bonded with aqueous solutions of some organic compounds containing 0.5–1.0 % boric acid.

Now we are developing this new technology for making sandwiches, which will not use the SPS method, but will take the product of required profile under pressure and then sinter/consolidate it using traditional pressureless methods. In this case, it is necessary to use binders to form a raw product. Encouraging preliminary results have been obtained using organic polymer solutions for binding material.

In this approach, expensive finely dispersed commercial powders can be replaced by the commercially available reagents. Boron carbide and multicomponent powders of its composites should be received. Several reports have been already published on this issue. Here, these methods are used by us to obtain neutron capture materials. Their essence is briefly described below.

Target composites are obtained using inexpensive reagent: boric acid, tungsten, titanium and zirconium oxides, metal salts, and organic compounds, which represent a source of carbidizing amorphous carbon, as well as reductants. For example, preceramic precursors are obtained by pyrolysis of a paste made from ammonium paratungstate, zirconium oxide, cobalt acetate, sucrose and amorphous boron at 100–200 °C.

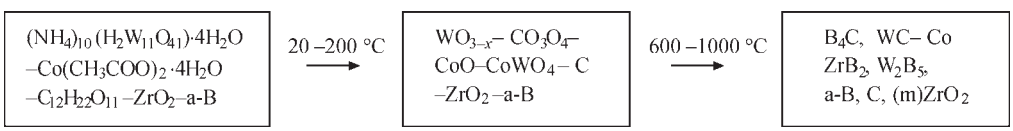

Figure 6. General scheme of obtaining preceramic precursors from mixture of zirconium(IV) oxide–ammonium paratungstenate–cobalt(II) acetate tetrahydrate–amorphous boron–sucrose

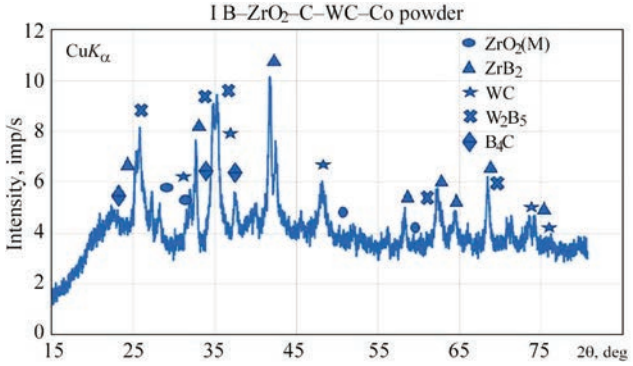

Figure 7. XRD pattern of preceramic precursor obtained from mixture of $(NH_4)_{10}(H_2W_{11}O_{41})\cdot 4H_2O$, $Co(CH_3COO)_2\cdot 4H_2O$, ZrO_2, B and $C_{12}H_{22}O_{11}$ at 1000 °C

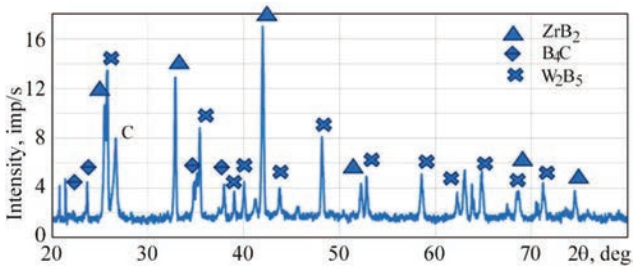

Figure 8. XRD pattern of composite obtained from preceramic precursors by SPS method at 1550 °C

General scheme of this example route is presented in Figure 6. The component phases (B_4C, ZrB_2, W_2B_5 and Co) are obtained by simple technology at relatively moderate temperatures: 800–1000 °C. So far, 1000 °C was the lowest temperature, at which the W_2B_5 phase formation was detected.

It is experimentally established that the starting compounds undergo the certain transformations upon gradual heating to 1000 °C (Figure 7). Raw products are made from preceramic precursors, and

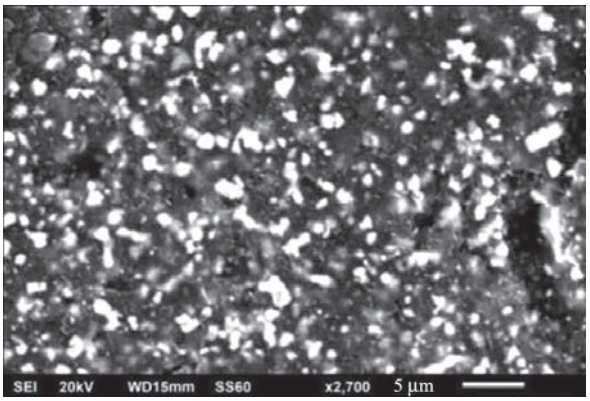

Figure 9. SEM micrograph of simple obtained from preceramic precursors by SPS method at 1700 °C

Figure 10. Raw sandwich made from preceramic precursor paste obtained from zirconium oxide–ammonium paratungstenate–cobalt acetate tetrahydrate–amorphous boron–sucrose system

neutron-capturing sandwiches are obtained by their annealing. It is important that composites containing boron carbide, tungsten boride and zirconium boride are obtained in a single technological process. Tungsten carbide and zirconium diboride (Figure 8), which are boron carbide particle growth inhibitors, are ob-

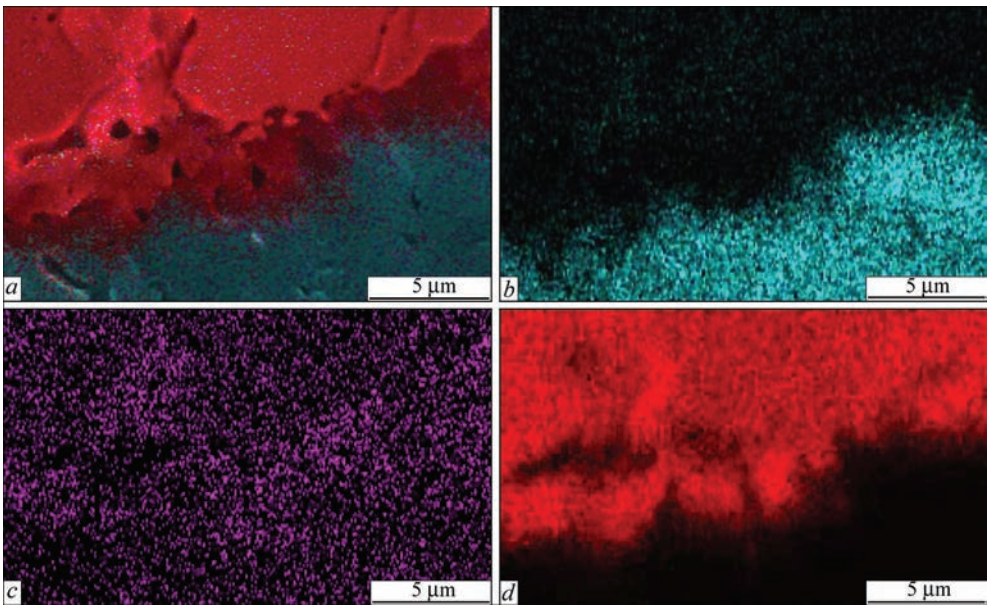

Figure 11. EDS mapping of (*a*) all elements in B_4C/W composite, and separately (*b*) B, (*c*) C and (*d*) W atoms distributions in B_4C and W phases contact regions, respectively

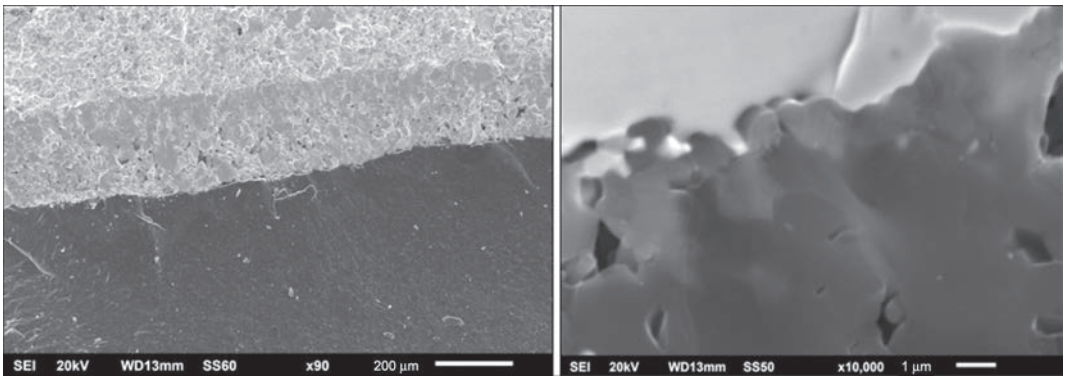

Figure 12. SEM images of fracture surfaces of B_4C–W composite obtained by SPS from B_4C and W powders at 1600 °C in magnifications of (*a*, ×90) and (*b*, ×10000)

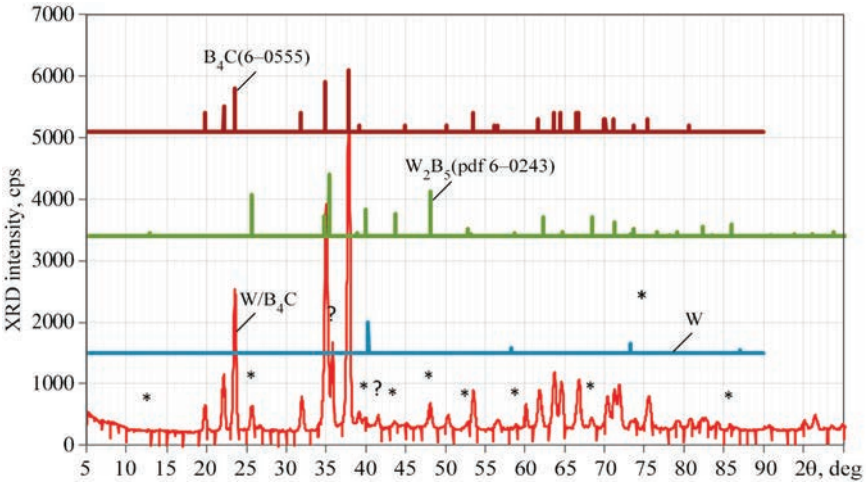

Figure 13. XRD pattern of B_4C–W_2B_5 composite obtained from B_4C–W_2B_5–W sandwich composite after selectively removing of metallic tungsten layer by treatment with hydrogen peroxide 30% solution, where peaks corresponding to B_4C and W_2B_5 component- and W trace-phases are shown separately

tained as intermediate products and contribute to boron carbide sintering.

It is interesting to note that the grains size of the composite are small, ranges within 0.5–2.0 μm (Figure 9) and practically does not change during annealing at 1700 °C. Raw sandwiches are obtained from similar preceramic powders (Figure 10). And by mixing them, B_4C–ZrB_2–W_2B_5 composite is formed, which is a promising material for neutron capture composites.

Preceramic precursors containing titanium and cobalt and boron carbide matrix ceramics are obtained in the same way. It is established that these sandwiches do not undergo exfoliation at the contact boundary of metal and boron carbides and, due to the physical-chemical processes taking place during the components sintering, are materials of high strength and hardness. From the EDS mapping images (Figure 11), it can be seen that at the phase boundary between tungsten and boron carbide (Figure 12) the diffusion of tungsten in the boron carbide layer and the formation of tungsten pentaboride take place (Figure 13). This phase is not detected after the tungsten layer selective removal.

CONCLUSIONS

The favorable properties of tungsten borides for shielding the spherical tokamak fusion power plant central HTS (High-Temperature Superconductor) core have been modelled [32] to minimize the power deposition into the cooled HTS core and to keep its radiation damage to acceptable levels by limiting the neutron and gamma fluxes. The shield materials compared are W_2B, WB, W_2B_5 and WB_4 along with a reactively sintered boride $B_{0.329}C_{0.074}Cr_{0.024}Fe_{0.274}W_{0.299}$, monolithic W and WC. Five shield thicknesses between 253 and 670 mm (corresponding to plasma major radii between 1400 and 2200 mm) are considered. W_2B_5 gives the most favorable results with reduction factor of > 10 in neutron flux and gamma energy deposition as compared to monolithic W. In particular, the W_2B_5 monolithic shields are found to have even better

performance than layered water-cooled ones, which is advantage from the safety perspective due to the risks associated with radio-activation of oxygen in water-cooled shields. The naturally occurring boron ^{10}B isotope 20% fraction gives much lower energy depositions than the 0% fraction, but the improvement largely saturates beyond 40 %. The performance of W_2B_5 is unrivalled by other monolithic shielding materials. This would be due to its trigonal crystal structure giving ^{10}B higher atomic density compared with other borides and, therefore, having just high enough content of ^{10}B to maintain a constant neutron energy spectrum across the shield.

Alternatively, effective radiation shields can be fabricated from tungsten composites with other boron compounds. For example, the tungsten–hexagonal boron nitride core–shell W@h-BN nanoparticles have been synthesized [33] by arc core discharge from tungsten atoms and borazine. The h-BN coats around the W-nanoparticles surface improving in this way their oxidation resistance. The fabricated 20 wt.% W@h-BN/BP-epoxy composite exhibits thermal neutron and gamma-ray shielding with absorption and attenuation coefficients of 3.51 and 0.357 cm^{-1}, respectively. These core–shell nanosystems can effectively shield not only the secondary γ rays emitted by thermal neutrons capture process of ^{10}B, but the primary γ rays as well. The W@h-BN-based materials can be utilized in space or extreme environments, where radiation shielding is critical for human activities.

Sandwich-structures of ^{10}B-enriched layers prepared by PLD (Pulsed Laser Deposition) serve [34] for development of novel neutron detectors showcasing improved efficiency, sensitivity and discrimination against γ background signals arisen from environment or neutron field.

In this work, the ^{10}B-based neutron capturing sandwich and multilayer structures are obtained using powder mixtures of compositions B_4C, B_4C–W and B_4C–W_2B_5. It is established that tungsten pentaboride phase is formed at the contact boundary between tungsten and boron carbide interfaces, which ensures component-layers strong bonding.

ACKNOWLEDGEMENT

Authors are thankful to the Republic Center for Structural Researches (GTU, Tbilisi, Georgia).

REFERENCES

1. Ozer, S.C., Buyuk, B., Tugrul, A.B. et al. (2016) Gamma and neutron shielding behavior of spark plasma sintered boron carbide-tungsten based composites. In: *Proc. of 145th Ann. Meeting Suppl. on TMS*, Cham, Springer Int. Publ., 449–456. DOI: https://doi.org/10.1002/9781119274896.ch54
2. Windsor, C.G., Astbury, J.O., Davidson, J.J. et al. (2021) Tungsten boride shields in a spherical tokamak fusion power plant. *Nucl. Fusion*, **61**, 086018 (1–14). DOI: https://doi.org/10.1088/1741-4326/ac4866
3. Chkhartishvili, L., Chedia, R., Tsagareishvili, O. et al. (2022) Preparation of neutron-capturing boron-containing nanosystems. In: *Proc.of 9th Int. Conf. on Exh. Adv. Nano Mater.*, Victoria, IAEMM, 1–15.
4. Chkhartishvili, L., Makatsaria, Sh., Gogolidze, N. (2023) Boron-containing fine-dispersive composites for neutron-therapy and neutron-shielding. In: *Proc.of Int. Sci. Prac. Conf. on Innov. Mod. Challen.–2022*, 2023, Tbilisi, Tech. Univ., 221–226.
5. Chkhartishvili, L., Makatsaria, Sh., Gogolidze, N. et al. (2023) Obtaining boron carbide and nitride matrix nanocomposites for neutron-shielding and therapy applications. *Condensed Matter*, 8(**4**), 92 (1–27). DOI: https://doi.org/10.3390/condmat8040092
6. Nabakhtiani, G., Chkhartishvili, L., Gigineishvili, A. at al. (2013) Attenuation of gamma-radiation concomitant neutron-absorption in boron–tungsten composite shields. *Nano Studies*, **8**, 259–266.
7. Chkhartishvili, L. (2018) Boron-contained nanostructured materials for neutron-shields. In: *Nanostructured Materials for the Detection of CBRN*. Eds by J. Bonca, S. Kruchinin. Dordrecht, Springer Science, Ch. 11, 133–154. DOI: https://doi.org/10.1007/978-94-024-1304-5_11
8. Evans, B.R., Lian, J., Ji, W. (2018) Evaluation of shielding performance for newly developed composite materials. *Ann. Nucl. Energy*, **116**, 1–9. DOI: https://doi.org/10.1016/j.anucene.2018.01.022
9. Park, J., Hossain, M.M., Jang, S.G., Kim, M.J. (2024) W@ boron nitride core-shell nanoparticles for radiation shielding. *ACS Appl. Nano Mater.*, 7(**9**), 10490–10497. DOI: https://doi.org/10.1021/acsanm.4c00888
10. Martin, P.M. (2018) Active thin films: Applications for graphene and related materials. *Vac. Technol. Coat.*, 19(**11**), 6–14.
11. Zinovev, A., Terentyev, D., Chang, C.-C. et al. (2022) Effect of neutron irradiation on ductility of tungsten foils developed for tungsten–copper laminates. *Nucl. Mater. Energy*, **30**, 101133 (1–10). DOI: doi.org/10.1016/j.nme.2022.101133
12. Sorokin, O., Kuznetsov, B., Lunegova, Y., Erasov, V. (2020) High-temperature composites with a multi-layered structure (Review). *Proc. All-Russian Sci. Res. Inst. Aviat. Mater.*, 88(**4–5**), 42–53 [in Russian].
13. Mann, K.S., Mann, S.S. (2021) Py-MLBUF: Development of an online-platform for gamma-ray shielding calculations and investigations. *Ann. Nucl. Energy*, **150**, 107845 (1–22). DOI: https://doi.org/10.1016/j.anucene.2020.107845
14. Dai, M., Zhang, Z., Zhu, J. et al. (2009) Influence of interface roughness on reflectivity of tungsten/boron-carbide multilayers with variable bi-layer number by X-ray reflection and diffuse scattering. *Chinese Opt. Lett.*, 7(**8**), 738–740. DOI: https://doi.org/10.3788/COL20090708.0738
15. Wang, Y., Long, B.F., Liu, C.Y., Lin, G.A. (2021) Evolution of reduction process from tungsten oxide to ultrafine tungsten powder via hydrogen. *High Temp. Mater. Proc.*, **40**, 171–177. DOI: https://doi.org/10.1515/htmp-2021-0017
16. Chang, M., Leung, C., Wang, D.N., Cheng, D. (1991) *Process for CVD deposition of tungsten layer on semiconductor wafer*. Pat. US, 5028565, July 2.
17. Kim, S.H. (1994) Deposition of tungsten thin film on silicon surface by low pressure chemical vapor deposition method. *J. Korean Chem. Soc.*, 38(**7**), 473–479.
18. Plyushcheva, S.V., Mikhailov, G.M., Shabel'nikov, L.G., Shapoval, S.Yu. (2009) Tungsten thin-film deposition on a silicon wafer: The formation of silicides at W–Si interface.

Inorg. Mater., **45**, 140–144. DOI: https://doi.org/10.1134/S002016850902006X
19. Kim, H.-J., Lee, J.-H., Sohn, I.-H. et al. (2002) Preparation of tungsten metal film by spin coating method. *Korea-Australia Rheol. J.*, 14(**2**), 71–76.
20. Yu, M.L., Ahn, K.Y., Joshi, R.V. (1990) Surface reactions in the chemical vapor deposition of tungsten using WF_6 and SiH_4 on Al, PtSi, and TiN. *J. Appl. Phys.*, **67**, 1055–1061. DOI: https://doi.org/10.1063/1.345791
21. Gao, J., Chan, L.H., Wongsenakhum, P. (2010) *Methods for improving uniformity and resistivity of thin tungsten films*. Pat. US, 7655567B1, February 2.
22. Yang, M., Aarnink, A.A.I., Kovalgin, A.Y. et al. (2016) Comparison of tungsten films grown by CVD and hot-wire assisted atomic layer deposition in a cold-wall reactor. *J. Vac. Sci. Technol. A*, 34(**1**), 01A129 (1–10). DOI: https://doi.org/10.1116/1.4936387
23. Dippel, A.-C., Schneller, T., Lehmann, W., Reichenberg, B., Waser, R. (2008) Tungsten coatings by chemical solution deposition for ceramic electrodes in fluorescent tubes. *J. Mater. Chem.*, **18**, 3501–3506. DOI: https://doi.org/10/1039/B802686F
24. Mallia, B., Dearnley, P. (2013) Exploring new W–B coating materials for the aqueous corrosion-wear protection of austenitic stainless steel. *Thin Solid Films*, **549**, 204–215. DOI: https://doi.org/10.1016/j.tsf.2013.09.035
25. Cao, P., Cao, J.-P., Cao, J.-H. (2021) *Boron carbide ceramic metallization preparation method*. Pat. CN, 110981550B, December 7[in Chinese].
26. Taran, A.V., Garkusha, I.E., Taran, V.S. et al. (2021) Structure and properties of B_4C coatings obtained by RF sputtering with external magnetic field. *Springer Proc. Phys.*, **246**, 51–57. DOI: https://doi.org/10.1007/978-3-030-51905-6_5
27. Barbakadze, N., Sarajishvili, K., Chedia, R. Et al. (2019) Obtaining of ultrafine powders of some boron carbide based nanocomposites using liquid precursors. *Nanotechnol. Percep.*, 15(**3**), 243–256. DOI: https://doi.org/10.4024/N27BA19A.ntp.15.03
28. Chkhartishvili, L., Mikeladze, A., Chedia, R. et al. (2020) Synthesizing fine-grained powders of complex compositions B_4C–TiB_2–WC–Co. *Solid State Sci.*, **108**, 106439 (1–8). DOI: https://doi.org/10.1016/j.solidstatesciences.2020.106439
29. Barbakadze, N., Chkhartishvili, L., Mikeladze, A. et al. (2022) Method of obtaining multicomponent fine-grained powders for boron carbide matrix ceramics production. *Mater. Today Proc.*, 51(**5**), 1863–1871. DOI: https://doi.org/10.1016/j.matpr.2021.08.013
30. Chkhartishvili, L., Mikeladze, A., Jalabadze, N. et el. (2022) New low-temperature method of synthesis of boron carbide matrix ceramics ultra-dispersive powders and their spark plasma sintering. *Solid State Phenom.*, **331**, 173–184. DOI: https://doi.org/10.4028/p-8n6hzy
31. Chkhartishvili, L., Mikeladze, A., Chedia, R. et al. (2022) Combustion synthesis of boron carbide matrix for superhard nanocomposites production. In: *Advances in Combustion Synthesis and Technology.* Eds by M. Bugdayci, L. Oncel. Singapore, Bentham Sci. Publ., Ch. 4, 66–95. DOI: https://doi.org/10.2174/9789815050448122010007
32. Windsor, C.G., Astbury, J.O., Davidson, J.J. et al. (2021) Tungsten boride shields in a spherical tokamak fusion power plant. *Nucl. Fusion*, **61**, 086018 (1–14). DOI: https://doi.org/10.1088/1741-4326/ac4866
33. Park, J., Hossain, M.M., Jang, S.G., Kim, M.J. (2024) W@boron nitride core-shell nanoparticles for radiation shielding. *ACS Appl. Nano Mater.*, 7(**9**), 10490–10497. DOI: https://doi.org/10.1021/acsanm.4c00888
34. Provenzano, Ch., Marra, M., Caricato, A.P. et al. (2023) Development of a high-efficiency device for thermal neutron detection using a sandwich of two high-purity ^{10}B enriched layers. *Sensors*, **23**, 9831 (1–11). DOI: https://doi.org/10.3390/s23249831

ORCID
L. Chkhartishvili: 0000-0003-3926-4524
N. Barbakadze: 0000-0002-5436-8009

CONFLICT OF INTEREST
The Authors declare no conflict of interest

CORRESPONDING AUTHOR
L. Chkhartishvili
Georgian Technical University
77 Merab Kostava Ave., 0160, Tbilisi, Georgia
E-mail: levanchkhartishvili@gtu.ge

SUGGESTED CITATION
L. Chkhartishvili, N. Barbakadze, O. Tsagareishvili, A. Mikeladze, O. Lekashvili, K. Kochiashvili, R. Chedia (2024) Neutron shield materials based on boron carbide–tungsten multilayer composites. *The Paton Welding J.*, **9**, 20–28.
DOI: https://doi.org/10.37434/tpwj2024.09.03

JOURNAL HOME PAGE
https://patonpublishinghouse.com/eng/journals/tpwj

Received: 01.08.2024
Received in revised form: 04.09.2024
Accepted: 07.10.2024